Bsr, a Nuclear-retained RNA with Monoallelic Expression^D

Hélène Royo,* Eugenia Basyuk,† Virginie Marty,* Maud Marques,*‡ Edouard Bertrand,† and Jérôme Cavaillé*

*Laboratoire de Biologie Moléculaire Eucaryote-Centre National de la Recherche Scientifique, Unité Mixte de Recherche 5095, Institut d'Exploration Fonctionnelle des Génomes 109, 31062 Cedex Toulouse, France; and †Institut Génétique Moléculaire Montpellier-Centre National de la Recherche Scientifique, Unité Mixte de Recherche 5535, Université Montpellier II, 34293 Montpellier Cedex 5, France

The imprinted *Dlk1-Gtl2* and Prader-Willi syndrome (PWS) regions are characterized by a complex noncoding transcription unit spanning arrays of tandemly repeated C/D RNA genes. These noncoding RNAs (ncRNAs) are thought to play an essential but still poorly understood role. To better understand the intracellular fate of these large ncRNAs, fluorescence in situ hybridization was carried out at the rat *Dlk1-Gtl2* domain. This locus contains a ~100-kb-long gene cluster comprising 86 homologous RBII-36 C/D RNA gene copies, all of them intron-encoded within the ncRNA gene *Bsr*. Here, we demonstrate that the Bsr gene is monoallelically expressed in primary rat embryonic fibroblasts as well as in hypothalamic neurons and yields a large amount of unspliced and spliced RNAs at the transcription site, mostly as elongated RNA signals. Surprisingly, spliced *Bsr* RNAs released from the transcription site mainly concentrate as numerous, stable nuclear foci that do not colocalize with any known subnuclear structures. On drug treatments, a fraction of *Bsr* RNA relocalizes to the cytoplasm and associates with stress granules (SGs), but not with P-bodies, pointing to a potential link between SGs and the metabolism of ncRNA. Thus, *Bsr* might represent a novel type of nuclear-retained transcript.

INTRODUCTION

Large-scale cDNA sequencing projects and systematic computational approaches have recently shown that an unexpected part of mammalian genomes is transcribed into RNA species lacking protein-coding potential and these transcripts—termed nonmessenger RNAs or noncoding RNAs (ncRNAs)—are now believed to represent a major component of the mammalian transcriptome (Carninci *et al.,* 2005; Cheng *et al.,* 2005 and references therein). Among these ncRNAs, a large fraction belongs to the so-called "mRNA-like" family that includes spliced, poly(A) RNAs without any conserved and statistically significant open reading frame (ORF). These enigmatic RNAs can be transcribed from intronic sequences, intergenic regions, or even from pseudogenes, and a substantial fraction of them is antisense to protein-coding genes or to other ncRNA genes (Yelin *et al.,* 2003; Katayama *et al.,* 2005). It has been hypothesized that ncRNAs might exert a key role in the regulation of eukaryotic gene expression (Mattick, 2004). However, their roles are a matter of debate, as it is still unclear whether they are all functional or whether they simply reflect spurious transcription.

Of particular interest is a growing list of recent results demonstrating the involvement of ncRNAs in a broad range of epigenetic regulatory pathways (Bernstein and Allis, 2005), including in mammalian systems X-chromosome inactivation and genomic imprinting. X-chromosome inactivation is a developmentally regulated process that silences nearly all the genes residing on one X-chromosome (Xi) in mammalian females. It is controlled by the X-inactivation center (Xic), from which the spliced, 17-kb-long *Xist* ncRNA is produced (Brockdorff *et al.,* 1992; Brown *et al.,* 1992). Remarkably, *Xist* "coats" the future inactive X chromosome (Clemson *et al.,* 1996) and initiates transcriptional gene silencing of nearly all the genes residing on it (Chow *et al.,* 2005). Genomic imprinting is an epigenetic regulation that leads to preferential expression of one of the two alleles according to its parental origin. Most of the imprinted genes are clustered in large chromosomal domains spreading over megabases, and their monoallelic expression, from the paternal or the maternal allele, is tightly coordinated by an intricate network of epigenetic features, including allele-specific DNA methylation and histone-tail modifications, differential timing of DNA replication, or subnuclear localization, as well as expression of large ncRNA genes (Reik and Walter, 2001; Gribnau *et al.,* 2003). Indeed, many imprinted ncRNA genes have been identified, with most of them expressed from the parental chromosome carrying neighboring, silent alleles of protein-coding genes (Sleutels and Barlow, 2002; O'Neill, 2005). Although their modes of action remain largely unknown, transcription of two of them, Air and Kcn1q0t1, and/or the ncRNAs per se are believed to be important for gene silencing (Sleutels *et al.,* 2002; Mancini-Dinardo *et al.,* 2006; Seidl *et al.,* 2006).
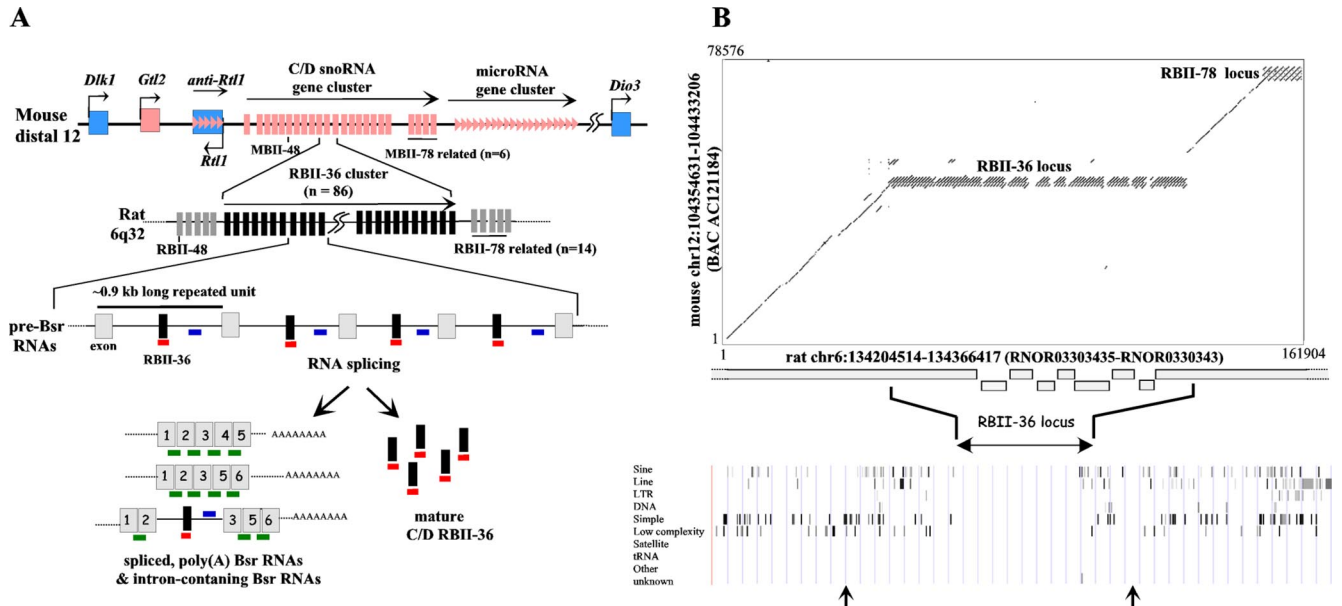
Figure 1. *Bsr* locus: a complex array of rat-specific, tandemly repeated C/D small nucleolar RNA (snoRNA) genes mapping at the imprinted *Dlk1-Gtl2* domain. (A) Schematic representation of the imprinted *Dlk1-Gtl2* domain. Top, the mouse distal 12 domain contains three paternally expressed protein-coding genes (*Dlk1, Rtl1,* and *Dio3*), depicted by blue boxes, and many maternally expressed noncoding RNA genes (*Gtl2,* miRNAs and C/D RNAs), symbolized by pink boxes, arrows, and bars, respectively. Middle, the rat locus contains an insertion of an ~100-kb-long region that consists of at least 86 direct tandem repeats (0.9 kb long), all of them spanning an intron containing the RBII-36 C/D RNA (vertical black bar) and one flanking ~80-nt-long exon without protein-coding potential (gray boxes). Bottom, *Bsr* locus generates a complex population of spliced, poly(A) RNA species (left) and fully mature RBII-36 C/D RNAs (right). DNA oligonucleotide probes are indicated by a green horizontal bar (spliced probe), a blue bar (intronic probe), and a red bar (RBII-36 probe). (B) Dot plot analysis of the rat C/D RNA gene cluster (6q32) versus the mouse C/D RNA gene cluster (distal 12). Top, mouse and rat sequences were retrieved from the Human Genome Project Working Draft (http://genome/ucsc.edu/), purged for common interspersed repeats with Repeat Masker (http://repeatmasker.genome.washington.edu/cgi-bin/RepeatMasker) and compared by Dot Plot analysis conducted by PipMaker program (http://bio.cse.psu.edu/). Bottom, repartition of the common interspersed sequences identified by the Repeat Masker software at http://genome/ucsc.edu/. Each bar represents a repeated or a low-complexity sequence, and the two arrows delineate the genomic sequences analyzed by Dot Plot. Note that the draft sequence of the rat genome at *Bsr* locus contains gaps.

The *Dlk1-Gtl2* is an evolutionary conserved, ~1-Mb imprinted chromosomal region lying on the distal arm of chromosome 12 in the mouse (corresponding to human 14q32 and rat 6q32; Figure 1A). It contains three protein-coding genes (*Dlk1, Rtl1,* and *Dio3*) that are only expressed from the paternal allele and multiple ncRNA genes that are only transcribed from the maternally inherited allele: 1) *Gtl2,* a large spliced and poly(A) RNA with multiple spliced isoforms (Schuster-Gossler *et al.,* 1998; Miyoshi *et al.,* 2000), 2) a poorly characterized antisense transcript to the *Rtl1* gene (Seitz *et al.,* 2003; Davis *et al.,* 2005), and 3) numerous small regulatory RNAs belonging to the C/D RNA and microRNAs (miRNAs) gene families known to direct site-specific RNA 2'O-methylations and silence gene expression at the posttranscriptional level, respectively (Kiss, 2002; Zamore and Haley, 2005). Many of these small RNA genes, whose functions are highly elusive (Davis *et al.,* 2005; Schratt *et al.,* 2006), are organized into clusters of repeated, homologous gene copies, with most of them embedded in and processed from introns of huge noncoding transcripts extending over several hundred kilobases (Cavaille *et al.,* 2002; Seitz *et al.,* 2004a). All the ncRNA genes are transcribed in the same orientation, with an apparently coordinated spatial-temporal expression pattern (Cavaille *et al.,* 2002; Seitz *et al.,* 2004a; Tierling *et al.,* 2006) and with an imprinted expression regulated by an intergenic, germline-derived, differentially methylated region (IG-DMR) located between *Dlk1* and *Gtl2* genes (Lin *et al.,* 2003). Thus, it is not formally known whether they are synthesized from their own promoters or

whether they are processed from a large, single transcription unit starting at the *Gtl2* promoter. Interestingly, the genomic organization of the C/D RNA gene cluster at the *Dlk1-Gtl2* domain, resembles the one at the imprinted Prader-Willi syndrome (PWS) chromosomal region, suggesting a functional and/or evolutionary link between repeated ncRNA genes and epigenetic imprinting processes (Cavaille *et al.,* 2000; reviewed in Seitz *et al.,* 2004b; Royo *et al.,* 2006).

The *Dlk1-Gtl2* domain has the potential to contribute to our understanding of imprinted ncRNA genes, either during development and/or upon epigenetic regulation. Indeed, mouse embryos that do not express the ncRNA genes die before the end of gestation and display many developmental abnormalities (Georgiades *et al.,* 2000; Lin *et al.,* 2003). Several microRNAs from processed anti-*RTL1* RNA direct RNA interference–mediated cleavages within the paternally expressed *RTL1* mRNA, whereas imprinted miR-134 inhibits the localized translation of limk1 mRNA at the synaptodendritic compartment of hippocampal neurons, highlighting the involvement of these small RNAs in the regulation of fetal growth and higher brain function, respectively (Davis *et al.,* 2005; Schratt *et al.,* 2006). Imprinted miRNAs are also suspected to be key players in polar overdominance phenomena, an unusual nonmendelian mode of inheritance described in sheep (Davis *et al.,* 2005). Finally, the lack of the expression of all the ncRNA genes on the maternal chromosome leads to the expression of genes that are normally maternally repressed (Lin *et al.,* 2003), raising the possibility

that ncRNAs might function to silence in *cis* the neighboring protein-coding genes.

To further understand these imprinted ncRNAs, we developed cell imaging approaches, to address yet unresolved issues regarding the metabolism of the large, spliced, C/D RNA host transcripts and their potential involvement in epigenetic regulation. We concentrated on the *Bsr* locus, a highly expressed transcription unit that encompasses a huge array of tandemly repeated C/D RNA genes (RBII-36) at the rat *Dlk1-Gtl2* domain. Several questions were specifically addressed: What is the intracellular fate of these large mRNA-like transcripts? Are they exported to the cytoplasm to be rapidly degraded by the nonsense-mediated RNA decay system (NMD)? Do they remain associated with their own parental locus like the chromosomal *Xist* RNA? Can any other roles be envisioned?

MATERIALS AND METHODS

Cell Cultures

Rat embryonic fibroblasts (REFs) were obtained from whole embryos freshly taken from female Wistar rats at 13–14 d of gestation. Embryos were dissociated chemically and mechanically and seeded in Dulbecco's modified Eagle's medium (DMEM) supplemented with 10% fetal calf serum, sodium pyruvate, and penicillin/streptomycin. Cells were cultivated at 37% in 5% CO_2. Primary hypothalamic neurons were prepared by mechanoenzymatic dissociation of fetal (E17) Wistar rat hypothalami as previously described in Shen *et al.* (1994). These primary cultures were routinely analyzed between days 8 and 14 after plating. For in situ hybridization, cells were plated on gelatin-coated (1%) 12-mm-diameter glass coverslips. REFs were either transiently transfected by using Lipofectamine 2000 (Invitrogen, Carlsbad, CA) or electroporated (Gene Pulser, Bio-Rad, Richmond, CA). Gene expression was routinely assayed 36–48 h after transfection. The mammalian expression vectors of GFP-H3 and YFP-PSP1α were generous gifts from Dr. P. Cook (University of Oxford) and from Dr. A. Lamond (University of Dundee), respectively, and the GFP-DCP1 and the GFP-G3BP plasmids were kindly provided by Dr. B. Séraphin (University of Paris 6, CNRS UPR 2167) and Dr. J. Tazi (IGMM, UMR 5535CNRS Montpellier), respectively. The GFP-MLBN1 plasmid and DMPK minigene were kindly provided by Dr. T. A. Cooper (Baylor College of Medicine, Houston, TX).

Fluorescence In Situ Hybridization

Fluorescence in situ hybridization (FISH) with DNA oligonucleotide probes was performed as described in http://singerlab.aecom.yu.edu/protocols/. In the case of DNA/RNA detection, DNA was heat-denatured (7 min at 85°C in 70% formamide, 2 × SSPE) before detection. The slides were then postfixed (10 min) before proceeding to RNA detection. Coverslips were mounted in Moviol DAPI (0.1 µg/ml). For in situ hybridization on rat brain sections, 10-µm cryosections were carried out. Fixation and hybridization on the sections were performed in the same conditions as those described above. Approximately 40–50 mer DNA oligonucleotide probes (Supplementary Data S5) were labeled with fluorolink Cy3 (Amersham Biosciences, Piscataway, NJ), Cy5 (Amersham Biosciences), or Oregon green (Molecular Probes, Eugene, OR). Images were captured with a CoolSnap ES camera (Roper Scientific, Tucson, AZ) mounted on a microscope (model DMRA, Leica, Deerfield, IL) with Leica 100× plan Apo 1.4 and using the Metavue software (Universal Imaging, West Chester, PA). 3D deconvolution was performed with Metamorph (Universal Imaging). The observations were confirmed by at least two of the authors.

Cell Fractionation and Ribonuclease A/T1 Protection Assay

Trypsinized REFs were suspended in nuclei buffer [0.25 M sucrose, 10 mM Tris, pH 7.4, 2.5 mM $MgCl_2$, 100 µg/ml collagenase (Sigma, St. Louis, MO), 2% Cemulsol NP10 (Rhône-Poulenc, a gift from J.-P. Zalta)] and disrupted with an Ultra-Turrax T25 basic (IKA-Werke, Staufen, Germany) (setting 2.7, 45 s). After 5 min of centrifugation (750 × g at 4°C), the supernatant was collected (= cytoplasmic fraction). The pellet was resuspended in nuclei buffer and disrupted again with Ultra-Turrax (setting 1.2, 30 s). Nuclei were then pelleted by centrifugation (5 min, 750 × g at 4°C), and RNAs were extracted with Trizol reagent (Invitrogen), whereas the cytoplasmic fraction was extracted twice with phenol/chloroform (saturated with water). Ribonuclease A/T1 protection assay (RPA) was performed according to standard protocol, with an internally ^{32}P-labeled 85-nt-long riboprobe complementary to the exon–exon junction.

RESULTS

A Complex Array of Repeated, C/D Small Nucleolar RNA Genes Embedded within Introns of Bsr, a Large ncRNA Gene

RBII-36 is a C/D RNA processed from tandemly repeated introns of *Bsr*, a large ncRNA gene encoded at the rat *Dlk1-Gtl2* domain (6q32 locus). The *Bsr* gene is mainly expressed in the brain (Komine *et al.*, 1999; Cavaille *et al.*, 2001) as well as in the placenta, the trunk of embryos (embryonic day E15.5), and REFs (not shown). This locus is remarkable as it gives rise, not only to the mature RBII-36 C/D RNA, but also to a large amount of spliced, poly(A) transcripts, as well as poorly characterized, unprocessed intron-containing RNA species (Figure 1A; Cavaille *et al.*, 2001). The *Bsr* locus has been predicted to be specific to the *Rattus* genus of rodents (Komine *et al.*, 1999; Cavaille *et al.*, 2001). The recent completion of the draft mouse and rat genomes allowed us to perform a more detailed sequence analysis. We now demonstrate unambiguously that the rat *Dlk1-Gtl2* locus contains an ~100-kb-long piece of DNA found neither in the mouse (Figure 1B), nor in any other available vertebrate genome and that this piece of DNA consists of at least 86 direct tandem repetitions of a 0.9-kb-long *Bsr* unit, spanning the entire C/D RNA-containing intron and one flanking ~80-nt-long, noncoding exon (Figure 1A). Given that the whole *Bsr* locus is almost devoid of common interspersed repeats, these observations point to recent gene amplification events that occurred probably after the divergence between mouse and rat. Thus, *Bsr* gene might represent another example of a brain-specific noncoding RNA that has evolved only in a specific lineage (Pollard *et al.*, 2006).

Monoallelic Expression at the Bsr Locus Is Resistant to TSA Treatment

We first checked whether *Bsr* gene is monoallelically expressed in REFs, by detecting simultaneously the *Bsr* locus with a mixture of four DNA oligonucleotide probes, designed to detect the template strand of *Bsr* repeated units (the DNA probes) and the nascent *Bsr* transcripts, the latter with an antisense DNA oligonucleotide probe designed to detect unspliced *Bsr* RNAs (the intronic probe). In 95.6% of the *Bsr*-expressing nuclei (n = 413), the intronic probe revealed only a single nuclear RNA signal overlapping one of the two DNA signals, thus demonstrating the monoallelic expression of the *Bsr* locus (Figure 2A). The remaining cells with two RNA signals mostly arise from large, tetra(poly)ploid nuclei (not shown), suggesting that *Bsr* monoallelic expression is unlikely to be regulated by a counting process. Monoallelic expression of the *Bsr* gene was also visualized in cultured primary neurons (prepared from the hypothalamus of E17 rat embryos) in which a single, nascent RNA signal was systematically detected in each nucleus of Tuj-positive neurons (Figure 2B), while only 5% of Tuj1-negative cells (mostly astrocytes as judged by their immunoreactivity with anti-GFAP antibodies, not shown), gave rise to weaker RNA signals at the transcription sites. The parental origin of the transcripts in REFs or neurons cannot be formally determined by our FISH protocol; however, we favor the hypothesis that the *Bsr* gene is expressed from the maternally inherited chromosome, as previously shown for the other surrounding ncRNA genes in the homologous imprinted mouse domain (Lin *et al.*, 2003).

The promoter sequences and RNA polymerase activities involved in *Bsr* gene transcription are unknown. However the sensitivity of *Bsr* gene expression to α-amanitin (20 µg/ml)
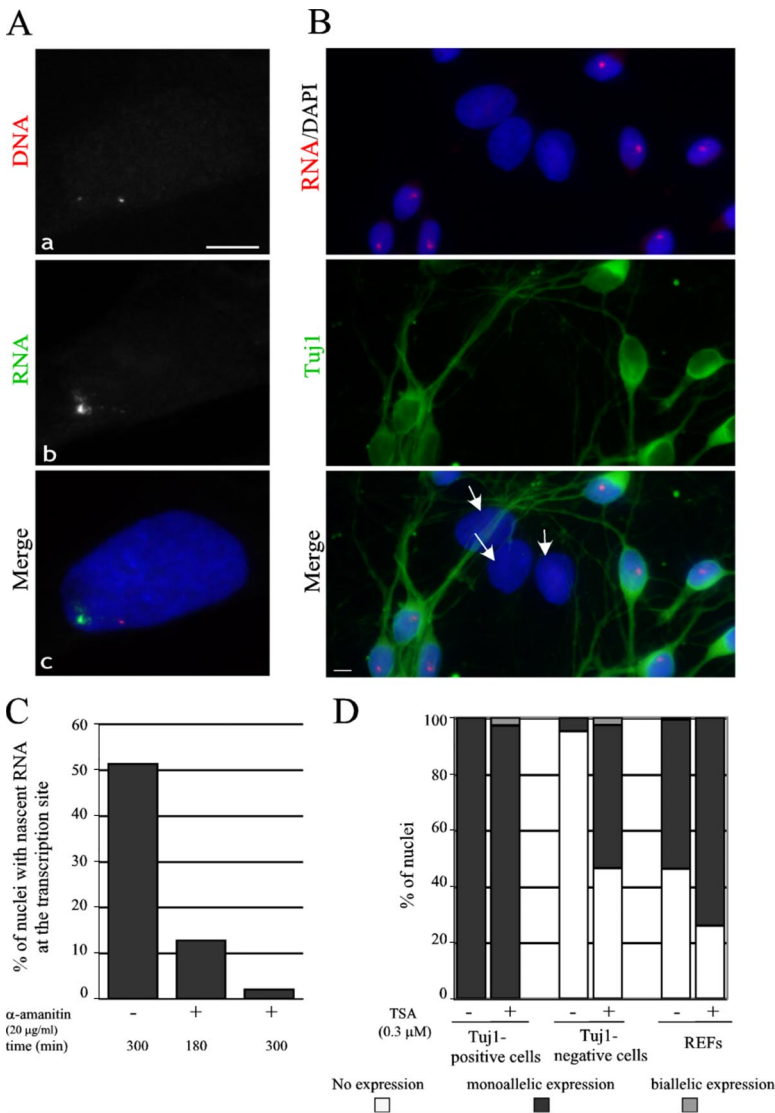
Figure 2. Monoallelic expression at the *Bsr* locus. (A) A representative REF nucleus simultaneously hybridized with the Cy3-labeled DNA probes (a) and the Oregon green–labeled intronic probe (b) to detect nascent transcripts. Nuclei were stained with DAPI. In some nuclei, very faint RNA signals around the second silent *Bsr* allele can sometimes be detected, probably due to the fact that the intronic probe can also hybridize to the DNA (not shown). Bar, 5 μm. (B) Monoallelic expression of *Bsr* is mainly restricted to neurons in E.17 primary rat hypothalamus cells. The panel shows a representative field of cultured primary hypothalamic neurons hybridized with a Cy3-labeled intronic probe (only a single nascent RNA signal is detected per nucleus) and stained by a monoclonal Tuj1 antibody to reveal neurons. Note that Tuj1-negative cells with larger nuclei (white arrows), most of which are astrocytes, do not express the *Bsr* gene. (C) Transcription of the *Bsr* gene is sensitive to α-amanitin. The percentage of nuclei with nascent RNAs at the transcription site (detected by the Cy3-labeled intronic probe) were scored in the control cells (−) and in the cells treated (+) by α-amanitin for 180 and 300 min (a minimum of 200 nuclei were analyzed). (D) Monoallelic expression at the *Bsr* locus is resistant to TSA treatment. Primary cultured hypothamic neurons or REFs were treated by TSA as indicated and the percentage of nuclei with none, one, or two transcription sites are indicated (a minimum of 200 nuclei were scored).

strongly suggests that RNA polymerase II is transcribing this large locus (Figure 2C).

Inhibitors of histone deacetylases, e.g., trichostatin A (TSA), can induce the reactivation of the normally silent allele at the *Igf2r* locus (Hu *et al.*, 2000). However, despite different experimental conditions (time courses ranging from 6 to 48 h and drug concentrations ranging from 0.3 to 3 μM), TSA treatments did not lead to any significant derepression of the silent *Bsr* allele (Figure 2D). Rather, the only significant change we reproducibly observed was an increase in the proportion of monoallelic expression in REFs or Tuj1-negative cells (from ~53 to 75% and from 5 to 50%, respectively; Figure 2D). Thus, the maintenance of monoallelic regulation at the *Bsr* locus is resistant to a drug that can affect the epigenetic state of chromatin.

Tracking the Intranuclear Fates of Noncoding RNAs Processed from the Bsr Locus

We next investigated the intracellular fates of the *Bsr*-associated transcripts by multicolor RNA FISH at the single nucleus level, by hybridizing simultaneously three fluorescent oligonucleotide probes: 1) an intronic-probe designed to detect unprocessed *Bsr* RNAs; 2) an RBII-36 probe de-

signed to detect the fully processed RBII-36 RNA and any other RBII-36–containing RNA precursor; and 3) a spliced-probe designed to recognize specifically the exon–exon junctions, thus allowing the specific detection of spliced *Bsr* RNA species. In agreement with data obtained in the adult rat brain sections (Supplementary Data S1), RBII-36 probe reveals the nucleolus as well as a strong and single nucleoplasmic signal that merges perfectly with that detected by the intronic probe, which never stains the nucleolus (Figure 3A, a, b, and e). Thus, the extranucleolar RBII-36 signal represents the nascent *Bsr* transcripts at the site of transcription. Interestingly, in many cases the intronic RNA signals exhibit a characteristic "comet-like" shape with a strong and compact signal ("the head") followed by weaker and more dispersed signals (one or two "tail(s)") as exemplified in Figure 3, A (right) and B (left). Surprisingly, in cells expressing high amounts of *Bsr*, the RBII-36 probe also detects dot-like signals relatively far away from the tail, as illustrated in Figure 3A (right). Although most of them seem to be organized in a nonrandom manner, with an apparent linear axis, no clear vectorial intranuclear trafficking from the tails of the comet toward the nucleolus, the nuclear interior, or the nuclear envelope was noticed. Because these
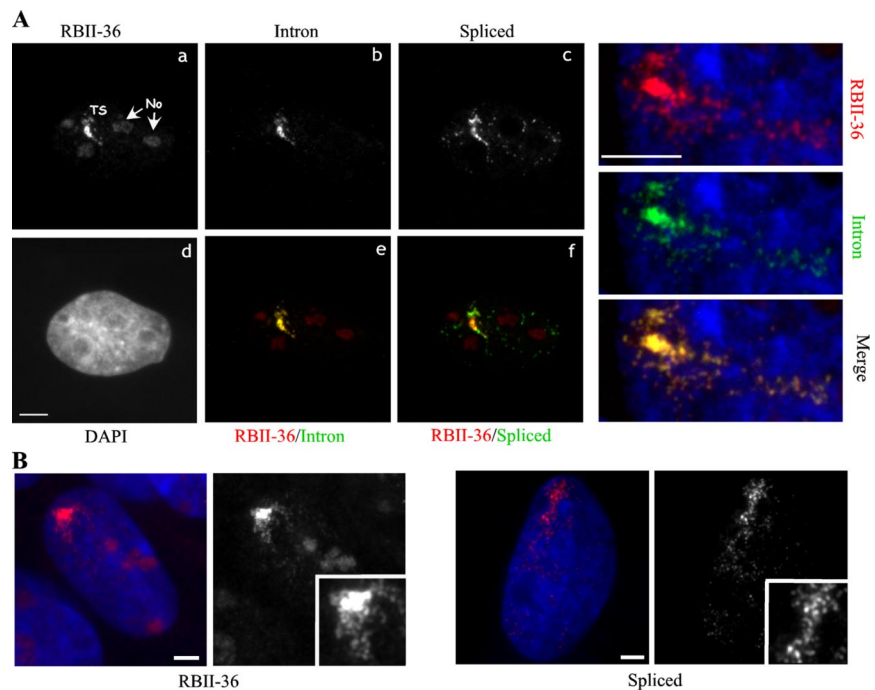
Figure 3. Tracking the intranuclear fate of the *Bsr*-derived transcripts. (A) Multicolor FISH at the single-cell level. Left, a representative nucleus hybridized with a Cy3-labeled RBII-36 probe (a), an Oregon-green–labeled intronic probe (b), and a Cy5-labeled spliced-probe (c) is shown. (e and f) Superimposition of panels a/b and panels a/c, respectively. Right, intron-containing *Bsr* precursors can be detected relatively far from the tails of the comet. (B) Characteristic large *Bsr* RNA signals at the transcription site. Representative "comet-like" (left) and "track-like" (right) RNA signals detected with Cy-3–labeled RBII-36 and spliced probes, respectively. Bars, 5 μm.

dot-like signals are also detected with the intronic-probe, they represent RBII-36 RNA precursors rather than fully mature RBII-36 RNAs traveling from their transcription site to the nucleolus.

The use of the spliced-probe also enables the visualization of nearly the same strong nuclear RNA signals detected by the intronic and the RBII-36 probes, although the observed signals are longer and more punctuated (Figure 3A, c and f, and B (right); see also Supplementary Data S2) with an average length of 7 ± 2 μm (n = 76 tracks) and an average area of 10 ± 5 μm^2, representing on average 1/27th (n = 72 cells) of the area of the nucleus. Very large RNA tracks can extend up to 13 μm and occupy up to 1/13th of the total nucleus (not shown). Even more interestingly, many bright, punctuated signals ("dot-like" RNA signals) whose number per nucleus could vary greatly (ranging from a few to 150–200, with an average of 38 dots per nucleus, n = 162 nuclei), were also systematically observed throughout the entire nucleoplasm but never within the nucleolus. In most cases, these dispersed, punctuated nuclear foci were not detected with the intronic probes (not shown), suggesting they likely represent fully (or nearly fully) spliced *Bsr* transcripts released from the transcription site. Finally, the same intranuclear fate of spliced *Bsr* RNAs, namely large RNA track and punctuated foci, was also observed in neurons (Supplementary Data S5A).

Spatial Relationships of Bsr-derived Transcripts in Relation to Their Locus and to Nuclear Architecture

Dual FISH to DNA and RNA was performed to address the question of whether there is a specific spatial relationship between the *Bsr* gene and these elongated RNA structures. Although heat denaturation affects to some extent the shape and the size of the RNA signals (not shown), in 83% of the examined nuclei (n = 58) the elongated nuclear RNA tracks and the comet-like signals extend beyond the side of the active *Bsr* allele, with the DNA signal positioned at one extremity within or even at the periphery of "the head" of the comet-like signals (Figure 4A). Remarkably, spliced *Bsr*

RNA signals do not perfectly superimpose with the intronic *Bsr* RNA signals. Indeed, whereas a gradient of decreasing intensity of the unspliced signals, from the head to the tail, is frequently observed, the intensity of the spliced *Bsr* signals is relatively equal all along the track-like signals or even increased in "the tails." These data are consistent with intronic RNA tracks belonging to nascent transcripts and/or partially processed *Bsr* RNA intermediates, whereas spliced RNA signals at the transcription site more likely reflect *Bsr* RNA molecules that are subjected to cotranscriptional RNA splicing and/or are recently released from DNA.

Most of the RNA signals detected by the spliced or the intronic probes fill up the regions of the nucleus that are poorly stained by DAPI, presumably reflecting their location in DNA-poor regions (Figure 4B, a and d; see also Supplementary Data S2). To confirm this, the location of spliced *Bsr* transcripts was analyzed in REFs transiently transfected by a plasmid expressing a green fluorescent protein (GFP)-tagged histone H3 that highlights the chromatin structure. Again, RNA signals at the transcription site, as well as those dispersed within the nucleoplasm, occupy nuclear regions that display low GFP signals (Figure 4B, b and d). Altogether, this is in agreement with observations indicating that nascent *Bsr* RNAs are released within the interchromatin space (Politz *et al.*, 1999; Verschure *et al.*, 1999; Politz and Pederson, 2000; Cremer *et al.*, 2004).

Bsr RNA Is a Nuclear-retained RNA That Does Not Colocalize with Known Nuclear Bodies

To unambiguously demonstrate that *Bsr* RNA species are mainly present in the nucleus, cell fractionation was carried out, and the relative amounts of spliced *Bsr* RNA species in the nucleus and in the cytoplasm fractions were examined by using a sensitive ribonuclease protection assay. As shown in Figure 5A, spliced *Bsr* RNAs were only recovered in the nuclear fraction. Thus, we conclude that spliced *Bsr* RNAs are unlikely to be exported significantly to the cytoplasm.

Several studies have reported the detection of poly(A) RNAs within SC-35 domains, the so-called nuclear speck-
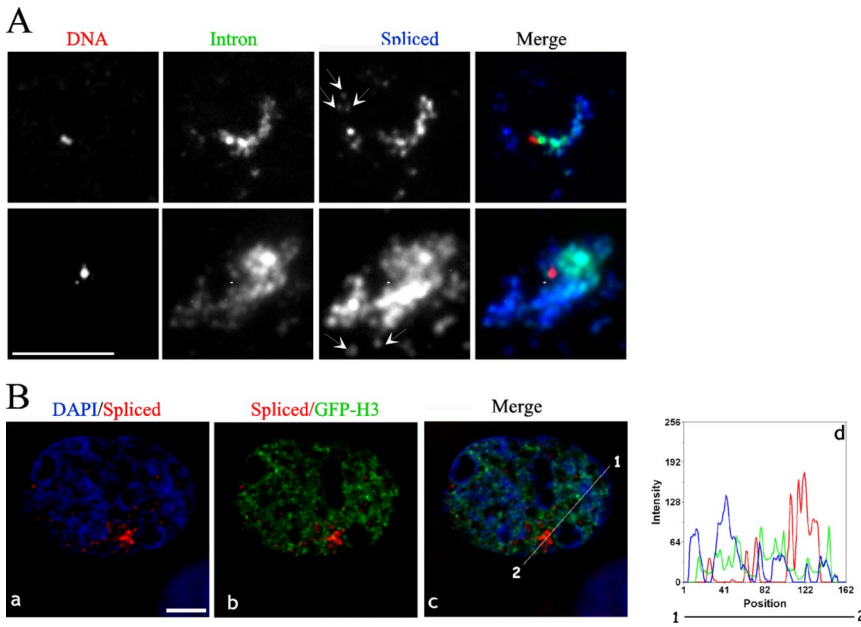
Figure 4. Spatial nuclear organization of the *Bsr* RNA tracks. (A) RNA splicing is spatially orientated along the elongated RNA track signals. Two representative transcription sites are shown. *Bsr* gene is detected by Cy3-labeled probes (red), the intron-containg *Bsr* RNAs by an Oregon green–labeled probe (green) and the spliced *Bsr* RNA by a Cy5-labeled probe (blue). Arrows indicate fully (or almost fully) spliced *Bsr* RNAs around the transcription site. (B) *Bsr* RNA tracks are restricted to the interchromosomal space. DNA- and chromatin-poor regions are visualized by DAPI staining (blue, a) and by GFP-H3 (green, b), respectively. A midplane from a deconvolved image stack is shown. (d) Fluorescence intensities of spliced *Bsr* RNA (red), DAPI (blue), and GFP-H3 (green) signals are plotted along the line as indicated in c. Note that spliced *Bsr* RNA signals are not significantly affected by DNAse I treatments, and they also resist high salt extraction (2 M NaCl/"halo preparation"; not shown). Bars, 5 μm.

les that are rich in components of the splicing machinery as well as other nuclear proteins (Lamond and Spector, 2003). Because these RNAs remain associated with speckles even in cells treated with transcriptional inhibitors, nucleus-restricted, poly(A) RNAs might contribute to organizing speckles (Huang *et al.*, 1994). We have consequently investigated the intranuclear distribution of the nuclear *Bsr* dots relative to the nuclear speckle domains revealed by GFP-SC35 staining. As shown in Figure 5B (top), *Bsr* dot-like do not accumulate preferentially within SC35 domains although ~70% are found at the edges of the speckles (n = 2439 dot-like analyzed). Similar nuclear staining patterns were also observed with speckles defined by U2 snRNPs (data not shown).

Paraspeckle domains are recently discovered nuclear bodies, usually found adjacent to speckles, that likely play a role in RNA synthesis and processing (Fox *et al.*, 2002). Interestingly, a nuclear-retained transcript—the CTN-RNA—has recently been shown to localize to paraspeckle domains (Prasanth *et al.*, 2005). As shown in Figure 5B (bottom), spliced *Bsr* RNA species are totally excluded from these nuclear structures as none of them overlap with the staining of a transiently transfected YFP-PSP1α or YFP-PSF (not shown), RNA-binding proteins enriched in paraspeckles. We thus conclude that *Bsr* RNA is neither a major component of the speckle, nor of the paraspeckle domains.

Transcripts from the mutant *DMPK* allele with expanded CUG repeats are retained in the nucleus and form multiple
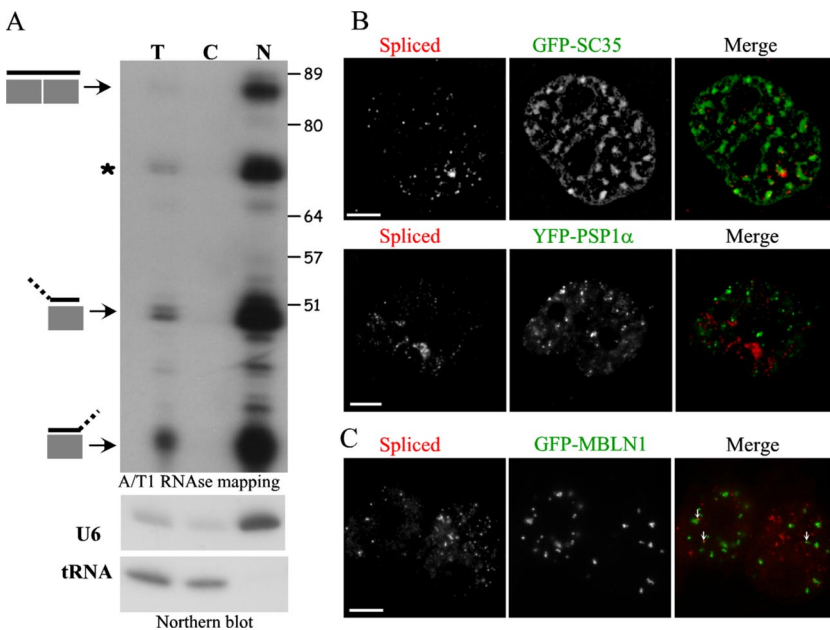

Figure 5. *Bsr* RNA, a novel nucleus-restricted poly(A) RNA. (A) Subcellular fractionation of REFs. Top, cytoplasmic versus nuclear fractions represent 81 versus 19% of the total, respectively. The same absolute amount of RNA (10 μg) was loaded in order to visualize enrichment in any fraction (cytoplasmic or nuclear) that would contain *Bsr* RNAs, compared with the input. Bottom, the quality of the fractions was checked by Northern blot using tRNA and U6 snRNA as cytoplasmic and nuclear markers, respectively. Note that the bands indicated by an asterisk (*) and those corresponding to hemi-protected *Bsr* exons can be due to alternative RNA splicing and/or sequence polymorphisms. Size (nt) is indicated. (B) Distribution of spliced *Bsr* RNA species relative to nuclear speckles (top) and paraspeckles (bottom) that are visualized by GFP-SC35 and YFP-PSP1α staining, respectively. To highlight speckle domains, pictures have been processed using a high-pass filter. Bar, 5 μm. (C) Distribution of spliced *Bsr* species relative to CUG-repeat foci made by mutant DMPK transcripts. REFs were transiently transfected with a mutant DMPK mini-gene containing 960 CUG repeats in its 3' untranslated region and a GFP-MBNL1–expressing plasmid. Expanded CUG repeat-containing transcripts form RNA foci are visualized by GFP-MBNL1 signals (green). Small white arrows indicate the few *Bsr* foci (detected by a Cy3-labeled probe, red) that overlap with those made by CUG foci.
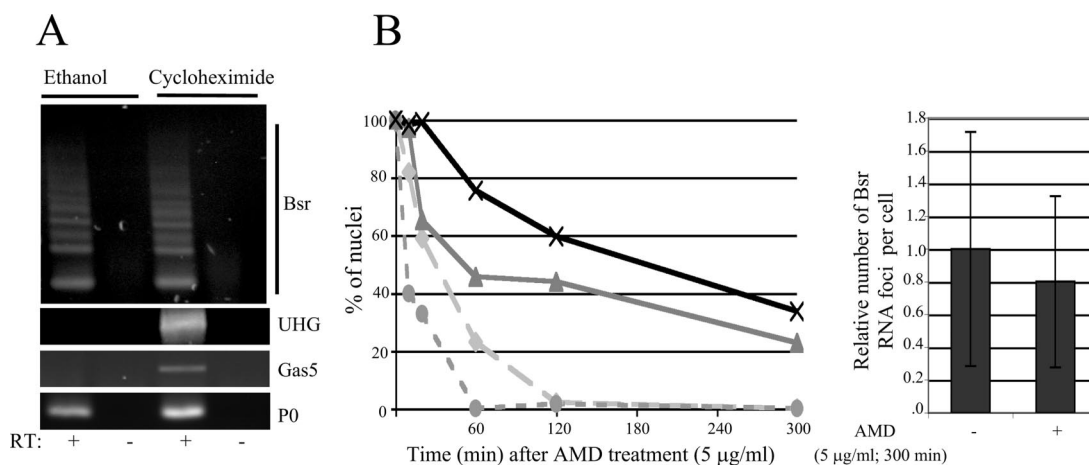
Figure 6. Effect of drug treatments on the stability of *Bsr*-derived transcripts. (A) Inhibition of protein synthesis does not affect the steady state of spliced *Bsr* RNAs. Cells were treated with cycloheximide (100 μg/ml) for 4 h. Total RNA was extracted, cDNA was synthesized with poly(dT) primers before amplification by PCR (n = 40 cycles) with specific primers for *Bsr*, gas5, UHG, and ribosomal protein P0 cDNAs (Supplementary Data S6). RT, reverse transcriptase. (B) Kinetics of the release of spliced- and intron-containing *Bsr* RNAs from the transcription site. Cells were treated with actinomycin D (5 μg/ml) for 10, 20, 60, 120, and 300 min before fixation and hybridization with either spliced probe or RBII-36 probe. Left, the proportion of nuclei with the RBII-36 RNA signals in the nucleoli ($\times$), the spliced RNA signals in nuclear dots ($\blacktriangle$), the intron-containing RNA signals at the transcription site ($\blacklozenge$), and the spliced RNA signals at the transcription site was assayed ($\bullet$). A time-course analysis is shown. A minimum of 100 nuclei was analyzed for each actinomycin D treatment. Right, analysis of the number of nuclear foci per cell in control cells (n = 112) and actinomycin D–treated cells (n = 109). The number of dot-like signals in control cells was set to 1.

discrete nuclear foci that recruit the muscleblind-like (MBNL1) proteins (Davis *et al.*, 1997; Ho *et al.*, 2005). The highly repeated exonic structure of spliced *Bsr* transcripts prompted to us to test the possibility that they might enter the same intranuclear pathway that prevents efficient export of mutant DMPK transcripts. To test this hypothesis, we analyzed the distribution of *Bsr* foci relative to those of CUG repeats foci. The intranuclear location of CUG repeat foci was visualized by cotransfecting REFs with a GFP-MNLB1 expression plasmid and with a *DMPK* minigene containing 960 CUG repeats. Consistent with previous results (Ho *et al.*, 2005), transcripts with CUG repeats recruit MNLB1 and induce the formation of punctate GFP-labeled CUG repeats (Figure 5C). Importantly, only a minority of those completely merge with foci containing spliced *Bsr* RNAs. We conclude from these observations that *Bsr* and CUG repeats foci do not occupy the same nuclear regions.

To gain further insights into the organization of these *Bsr* ribonuclear foci, a careful quantification analysis of the total fluorescence in individual dots was carried out. This analysis revealed that most of the *Bsr* nuclear dots contain a limited number of hybridized probes and supports the notion that they might correspond to single (or a few) RNA molecule(s) rather than clusters of multiple spliced *Bsr* RNAs attached to a putative nuclear structure (Supplementary Data S3).

Spliced Bsr RNAs Are Metabolically Stable Transcripts

Although we provide compelling evidence that spliced *Bsr* RNAs are mainly present in the nucleus, one could argue that *Bsr* RNAs are exported to the cytoplasm and then rapidly degraded by the NMD system, a quality control mechanism that eliminates transcripts carrying nonsense mutations. This process, which requires ongoing translation, is inhibited by protein synthesis inhibitors. Therefore, if *Bsr* RNAs enter the NMD pathway, their level of expression should increase when translation is halted. To test this hypothesis, REFs were treated with the translation elongation

inhibitor cycloheximide, and the level of *Bsr* RNAs was analyzed. As shown in Figure 6A, no change in the steady state of *Bsr* RNAs was observed upon treatment with cycloheximide, whereas the steady state of two noncoding C/D RNA host transcripts used as positive controls, UHG and gas5 RNAs, was dramatically increased in agreement with previous reports (Tycowski *et al.*, 1996; Smith and Steitz, 1998). As expected, no change was seen with the P0 ribosomal protein-coding mRNA. These data are consistent with spliced *Bsr* RNA being immune to NMD, most likely because it mainly remains within the nucleus.

The relative stability of the nuclear *Bsr*-derived transcripts was also evaluated by treating REFs with a high concentration of actinomycin D (5 μg/ml), a drug that acts very rapidly in vivo as a transcription inhibitor of all RNA polymerases. Qualitative analysis by RNA FISH revealed that actinomycin D treatment induces a relatively rapid release of spliced *Bsr* RNA species from the transcription site, with no nuclei exhibiting an obvious track-like structure after 60 min of incubation (Figure 6B, left, and Supplementary Figure S4B). However, during the same time-course experiment, the nuclear *Bsr* RNA dots dispersed throughout the nucleoplasm remain visible in a substantial fraction of the cells, and the number of Bsr RNA foci per cell is only slightly altered even after longer treatments (Figure 6B, right). The stability of these dot-like signals was also confirmed by treating cells with α-amanitin (data not shown). The use of the RBII-36 probes also shows that nucleolar RNA signals are nearly unaltered, consistent with RBII-36 being incorporated into metabolically stable RNPs (Figure 6B, left). From these data, we conclude that nuclear spliced *Bsr* RNAs are relatively stable transcripts and that *Bsr* foci are unlikely to represent nuclear sites of rapid degradation.

Cytoplasmic Bsr RNAs Associate with Stress Granules But Not with P-Bodies

The vast majority of spliced *Bsr* RNA signals are detected in the nucleus. However limited but significant dot-like signals
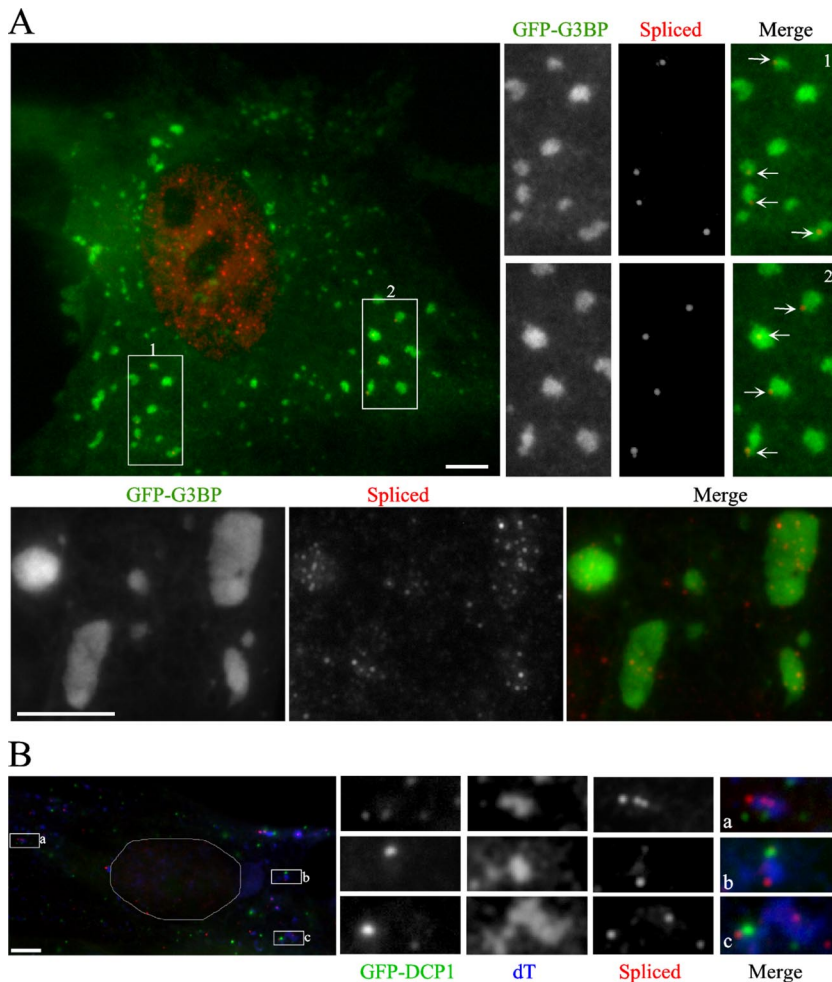
A

GFP-G3BP   Spliced   Merge

GFP-G3BP   Spliced   Merge

B

GFP-DCP1   dT   Spliced   Merge

Figure 7. Cytoplasmic *Bsr* RNAs associate with arsenite-induced stress granules. (A) REFs were transiently transfected with a GFP-G3BP expression plasmid, and stress granules were induced by arsenite treatment (0.5 mM for 30 min). Top, a representative cell is shown (left), the cytoplasm of which contains eight dot-like signals. The two boxes (termed 1 and 2) indicate the position of the enlarged fields (right). The contrasts have been enhanced to highlight *Bsr* dots (white arrows). Bottom, several large SGs that contain multiple spliced *Bsr* RNAs are shown. SGs are visualized by GFP-G3BP (green), and spliced *Bsr* RNAs are detected by a Cy3-labeled probe (red). (B) Cytoplasmic *Bsr* RNAs are not detected in P-bodies. A representative arsenite-treated REF is shown (left) with three boxes (termed a, b, and c) indicating the position of the enlarged fields (right) showing spliced *Bsr* RNA containing-SGs juxtaposed to PBs. PBs and SGs are visualized by DCP1-GFP (green) and poly(A) RNA signals with a Cy5-labeled poly(dT) probe (blue), respectively, whereas spliced *Bsr* RNAs are detected by a Cy3-labeled probe (red). The outline of the nucleus is indicated according to DAPI staining. For unknown reasons, nuclear *Bsr* staining and poly(A+) staining are altered in some arsenite-treated cells. Bars, 5 μm.

were observed in the cytoplasm of REFs and also in the dendritic compartments of hypothalamic neurons (Supplementary Data S5A). In REFs, their detection was highly variable, either in individual cells (partial or nearly total cytoplasmic relocation) or within the cell population (ranging from 1 to 12% of the cell population). Remarkably, a ~2–10-fold increase in the proportion of REFs with cytoplasmic *Bsr* RNA signals was noticed during the course of actinomycin D treatment or after various drug treatments, as well as to some extent after electroporation or liposome-mediated transfections (Supplementary Data S4). These observations argue in favor of a mechanism occurring in normal conditions that retains *Bsr* RNAs in the nucleus. We reasoned that this leak of *Bsr* from the nucleus to the cytoplasm might result from a global cellular stress.

In response to environmental stresses, 40S ribosome-associated poly(A)+ mRNA accumulate into translationally silent mRNP complexes within discrete cytoplasmic structures, the so-called stress granules (SGs; Kedersha and Anderson, 2002; Kedersha *et al.*, 2005). We therefore asked whether *Bsr* cytoplasmic RNAs accumulate in SGs by analyzing their distribution in REFs transiently transfected by a plasmid expressing the GFP-tagged G3BP endoribonuclease, a protein recruited to SGs under stress conditions (Tourriere *et al.*, 2003). As shown in Figure 7A (top), 67% of cytoplasmic *Bsr* signals were found associated with arsenite-induced SGs, many of them being detected at their close periphery (n = 384 cytoplasmic foci analyzed). To avoid any bias or

artifacts, only unambiguous cytoplasmic *Bsr* dots within cells displaying a moderate level of GFP signals were scored. Indeed, very large SGs, probably due to G3BP overexpression, frequently contain multiple *Bsr* RNA dots (up to 18, as illustrated in Figure 7A, bottom). A preferential association of *Bsr* RNAs within SGs was also observed in untransfected, arsenite-treated hypothalamic neurons, thus excluding the possibility that relocation of *Bsr* in SGs is simply due to GFP-G3BP expression (Supplementary Data S5B). To our knowledge, this is the first evidence that untranslated mRNAs can be present in SGs.

Processing bodies (PBs) constitute other specialized cytoplasmic compartments enriched in factors required for translational repression and 5′ to 3′ RNA decay (Eulalio *et al.*, 2007). Because SGs are often juxtaposed with PBs, mRNAs destined for degradation might be sorted in SGs and then routed to P-bodies as proposed earlier (Kedersha *et al.*, 2005). We addressed this hypothesis by simultaneously revealing PBs and SGs by GFP-DCP1 staining and hybridization to a Cy5-labeled oligo-dT probe to detect poly(A+) RNA species, respectively. As shown in Figure 7B, *Bsr* RNA species do not significantly colocalize with PBs (6% overlap) in arsenite-treated REFs (n = 1340 cytoplasmic dot-like signals analyzed). Reinforcing this notion, even in the case of *Bsr*-containing SGs positioned adjacent to PBs, no obvious overlap between *Bsr* foci and GFP-DCP1 signals was observed, again indicating that *Bsr* RNAs are unlikely to be targeted to PBs. The lack of detection of *Bsr* RNA signals

within PBs is unlikely to reflect their rapid 5′ to 3′ degradation in these bodies, because cytoplasmic *Bsr* RNAs are still detected after actinomycin D treatment (Supplementary Data S4).

DISCUSSION

Imprinted ncRNA genes are believed to play a role in genomic imprinting control and/or in the regulation of embryonic growth. However, their large size, their weak level of expression and their low sequence conservation have considerably limited their functional analysis (Sleutels *et al.,* 2002; Thakur *et al.,* 2004; O'Neill, 2005) and except for Xist (Clemson *et al.,* 1996), their intranuclear trafficking has not been extensively documented so far. In this report, the imprinted *Dlk1-Gtl2* domain was chosen as a model to further characterize the metabolism of large spliced C/D RNA host-gene transcripts synthesized and processed from the rat *Bsr* locus (Figure 1). Indeed, ncRNAs at the *Dlk1-Gtl2* domain are believed to play an important role during development (Georgiades *et al.,* 2000; Lin *et al.,* 2003; Davis *et al.,* 2005; Schratt *et al.,* 2006). In addition, its highly repeated gene organization and its high level of expression make the *Bsr* locus an appropriate cellular model with which to address, through cell imaging approaches, key questions regarding the intracellular fate of imprinted ncRNAs.

By using a FISH-based protocol with specific oligonucleotide probes conjugated to fluorochromes, we visualized the monoallelic expression of the *Bsr* gene at the single-cell level (Figure 2) and successfully tracked *Bsr*-derived transcripts, from the transcription site to the interchromatin space (Figures 3–5) and also to some extent in the cytoplasm including within dendrites of hypothalamic neurons (Figure 7, Supplementary Data S5). We showed that an unexpected large amount of spliced (or partially spliced) *Bsr* RNA signals accumulate in close proximity to its own locus (Figures 3 and 4). *Bsr* and *Xist* RNAs share some similar features in that they are monoallelically expressed genes that give rise to nuclear spliced, polyadenylated ncRNAs with many repeated sequence motifs. Repetitive sequences are known to attract gene silencing and the lack of expression of maternally expressed ncRNA genes at the *Dlk1-Gtl2* domain is associated with the reactivation of the neighboring, silent protein-coding genes (Lin *et al.,* 2003). Thus, and even though *Bsr* RNA species do not stably remain associated with their own locus (Figure 6) and they disappear during mitosis (not shown), these large nuclear RNA tracks around the transcription site might be the counterpart of the *Xist* RNA coating (Chow *et al.,* 2005). This notion is reinforced because we have found that two other imprinted ncRNA gene loci also generate large RNA accumulation around their transcription sites (Royo and Cavaillé, unpublished data).

Alternatively, spliced *Bsr* RNAs at the transcription site might reflect cotranscriptional RNA splicing and/or RNA splicing taking place immediately thereafter, as suggested by the spatially organized RNA splicing along the tracks (Figure 4). Although it is not well understood why many *Bsr* RNA signals display an elongated shape with a polar orientation relative to their gene, our observations strongly recall linear RNA signals previously observed for a few viruses and cellular protein-coding transcripts (Lawrence *et al.,* 1989; Xing *et al.,* 1993; Dirks *et al.,* 1995; Melcak *et al.,* 2000). One can intuit that a large amount of RNAs at the transcription site might result from any rate-limiting step between transcription and the subsequent intranuclear RNA trafficking. A correlation between the extent of RNA splicing and the presence of tracks has been noticed (Dirks *et al.,* 1995), and transcripts that are deficient in RNA processing are retained near the transcription site (Custodio *et al.,* 1999). Thus, inefficient splicing of *Bsr* pre-RNAs might account for its localized nuclear accumulation. It should be emphasized, however, that the cotranscriptional hypothesis is not mutually exclusive of an involvement of *Bsr* RNAs in gene silencing by still unknown mechanisms, either in the maintenance and/or the establishment of imprinted regulation at the Dlk1-Gtl2 domain. Indeed, no stable accumulation of Air or Kcnq1ot1 RNAs at their parental chromosome has been noticed so far (Sleutels *et al.,* 2002; Mancini-Dinardo *et al.,* 2006; Seidl *et al.,* 2006).

We have also made the surprising finding that *Bsr* RNAs released from the transcription site concentrate mostly in the interchromatin space as multiple, metabolically stable nuclear foci, rather than being rapidly exported to the cytoplasm as expected for spliced, polyadenylated RNAs. To our knowledge, nuclear RNA foci have only been well documented for two endogenously expressed, mammalian cellular transcripts: 1) the mutant *DMPK* alleles with expanded CUG trinucleotide repeats (Davis *et al.,* 1997) and 2) the recently discovered CTN-RNA that localizes to paraspeckles (Prasanth *et al.,* 2005). Remarkably, the intranuclear fate of *Bsr* transcripts differs considerably from that of these two nuclear-restricted transcripts (Figure 5) and above all dramatically contrasts with the other noncoding C/D RNA host gene transcripts, like Gas5 or UHG, which are short-lived transcripts associated with polysomes (Tycowski *et al.,* 1996; Smith and Steitz, 1998). These observations strongly argue against the possibility that *Bsr* transcripts simply correspond to "RNA remnants" of the spliced host transcripts that are undergoing nuclear RNA degradation. The mechanisms underlying the nuclear retention of spliced *Bsr* RNAs and their potential functions have not yet been identified.

Although our study unambiguously demonstrates that *Bsr* RNA represents a novel nuclear-retained RNA, a cytoplasmic function could also be envisioned. First, a small subfraction of *Bsr* RNAs can escape the nucleus and are targeted to the dendritic compartments of hypothalamic neurons (Supplementary Data S5A). Remarkably, miR-134, whose gene maps downstream from the *Bsr* locus, also localizes to the synapto-dendritic compartment of rat neurons wherein it controls the growth of dendritic spines (Schratt *et al.,* 2006). Whether the dendritic location of *Bsr* RNA reflects its involvement in the same cellular regulatory pathway is an intriguing question. Second, stress stimuli favor a relocation of *Bsr* RNAs in the cytoplasm, many of the transcripts being found within or in close proximity to SGs but not within PBs (Figure 7). SGs are thought to represent the sites of accumulation of stalled translation preinitiation complexes (Kedersha and Anderson, 2002). Thus this observation was largely unexpected because *Bsr* RNA does not contain any obvious protein-coding potential. The intracellular behavior of two other nuclear-retained RNAs is also altered upon a cellular stress: CTN-RNA is cleaved and released to the cytoplasm (Prasanth *et al.,* 2005), whereas heat shock causes Hsr-omega RNA-containing nuclear speckles to coalesce into larger clusters (Prasanth *et al.,* 2000). In addition, several noncoding RNAs are specifically induced and/or play a role in response to oxidative stress (Crawford *et al.,* 1996a,b; Wang *et al.,* 1996) or heat shock (Jolly *et al.,* 2004; Shamovsky *et al.,* 2006). Therefore, *Bsr* RNAs might sequester nuclear RNA-binding proteins and serve as storage sites that modulate their intracellular availability, depending on environmental and/or internal stimuli. Alternatively, because SGs contain endoribonuclease activities (Tourriere *et al.,* 2003), the possibility that *Bsr* RNAs

might undergo slow decay in these bodies cannot be formally excluded. More sophisticated experiments are now required to fully appreciate the potential interplay between ncRNAs and the function and/or the organization of the SGs.

Nuclear poly(A)$^+$ RNA species have been reported (Perry *et al.*, 1974; Carter *et al.*, 1991; Visa *et al.*, 1993; Huang *et al.*, 1994), and taking into account that noncoding RNAs represent a major outcome of mammalian transcripts (Carninci *et al.*, 2005; Cheng *et al.*, 2005), many other nuclear RNAs with roles in various aspects of nuclear functions and/or cell organization are expected to be described in the near future.

ACKNOWLEDGMENTS

REFERENCES

Bernstein, E., and Allis, C. D. (2005). RNA meets chromatin. Genes Dev. *19*, 1635–1655.

Brockdorff, N., Ashworth, A., Kay, G. F., McCabe, V. M., Norris, D. P., Cooper, P. J., Swift, S., and Rastan, S. (1992). The product of the mouse Xist gene is a 15 kb inactive X-specific transcript containing no conserved ORF and located in the nucleus. Cell *71*, 515–526.

Brown, C. J., Hendrich, B. D., Rupert, J. L., Lafreniere, R. G., Xing, Y., Lawrence, J., and Willard, H. F. (1992). The human XIST gene: analysis of a 17 kb inactive X-specific RNA that contains conserved repeats and is highly localized within the nucleus. Cell *71*, 527–542.

Carninci, P. *et al.* (2005). The transcriptional landscape of the mammalian genome. Science *309*, 1559–1563.

Carter, K. C., Taneja, K. L., and Lawrence, J. B. (1991). Discrete nuclear domains of poly(A) RNA and their relationship to the functional organization of the nucleus. J. Cell Biol. *115*, 1191–1202.

Cavaille, J., Buiting, K., Kiefmann, M., Lalande, M., Brannan, C. I., Horsthemke, B., Bachellerie, J. P., Brosius, J., and Huttenhofer, A. (2000). Identification of brain-specific and imprinted small nucleolar RNA genes exhibiting an unusual genomic organization. Proc. Natl. Acad. Sci. USA *97*, 14311–14316.

Cavaille, J., Seitz, H., Paulsen, M., Ferguson-Smith, A. C., and Bachellerie, J. P. (2002). Identification of tandemly-repeated C/D snoRNA genes at the imprinted human 14q32 domain reminiscent of those at the Prader-Willi/Angelman syndrome region. Hum. Mol. Genet. *11*, 1527–1538.

Cavaille, J., Vitali, P., Basyuk, E., Huttenhofer, A., and Bachellerie, J. P. (2001). A novel brain-specific box C/D small nucleolar RNA processed from tandemly repeated introns of a noncoding RNA gene in rats. J. Biol. Chem. *276*, 26374–26383.

Cheng, J. *et al.* (2005). Transcriptional maps of 10 human chromosomes at 5-nucleotide resolution. Science *308*, 1149–1154.

Chow, J. C., Yen, Z., Ziesche, S. M., and Brown, C. J. (2005). Silencing of the Mammalian x chromosome. Annu. Rev. Genom. Hum. Genet. *6*, 69–92.

Clemson, C. M., McNeil, J. A., Willard, H. F., and Lawrence, J. B. (1996). XIST RNA paints the inactive X chromosome at interphase: evidence for a novel RNA involved in nuclear/chromosome structure. J. Cell Biol. *132*, 259–275.

Crawford, D. R., Schools, G. P., and Davies, K. J. (1996a). Oxidant-inducible adapt 15 RNA is associated with growth arrest- and DNA damage-inducible gadd153 and gadd45. Arch. Biochem. Biophys. *329*, 137–144.

Crawford, D. R., Schools, G. P., Salmon, S. L., and Davies, K. J. (1996b). Hydrogen peroxide induces the expression of adapt15, a novel RNA associated with polysomes in hamster HA-1 cells. Arch. Biochem. Biophys. *325*, 256–264.

Cremer, T., Kupper, K., Dietzel, S., and Fakan, S. (2004). Higher order chromatin architecture in the cell nucleus: on the way from structure to function. Biol. Cell *96*, 555–567.

Custodio, N., Carmo-Fonseca, M., Geraghty, F., Pereira, H. S., Grosveld, F., and Antoniou, M. (1999). Inefficient processing impairs release of RNA from the site of transcription. EMBO J. *18*, 2855–2866.

Davis, B. M., McCurrach, M. E., Taneja, K. L., Singer, R. H., and Housman, D. E. (1997). Expansion of a CUG trinucleotide repeat in the 3' untranslated region of myotonic dystrophy protein kinase transcripts results in nuclear retention of transcripts. Proc. Natl. Acad. Sci. USA *94*, 7388–7393.

Davis, E., Caiment, F., Tordoir, X., Cavaille, J., Ferguson-Smith, A., Cockett, N., Georges, M., and Charlier, C. (2005). RNAi-mediated allelic trans-interaction at the imprinted Rtl1/Peg11 locus. Curr. Biol. *15*, 743–749.

Dirks, R. W., Daniel, K. C., and Raap, A. K. (1995). RNAs radiate from gene to cytoplasm as revealed by fluorescence in situ hybridization. J. Cell Sci. *108*(Pt 7), 2565–2572.

Eulalio, A., Behm-Ansmant, I., and Izaurralde, E. (2007). P bodies: at the crossroads of post-transcriptional pathways. Nat. Rev. Mol. Cell Biol. *8*, 9–22.

Femino, A. M., Fay, F. S., Fogarty, K., and Singer, R. H. (1998). Visualization of single RNA transcripts in situ. Science *280*, 585–590.

Fox, A. H., Lam, Y. W., Leung, A. K., Lyon, C. E., Andersen, J., Mann, M., and Lamond, A. I. (2002). Paraspeckles: a novel nuclear domain. Curr. Biol. *12*, 13–25.

Georgiades, P., Watkins, M., Surani, M. A., and Ferguson-Smith, A. C. (2000). Parental origin-specific developmental defects in mice with uniparental disomy for chromosome 12. Development *127*, 4719–4728.

Gribnau, J., Hochedlinger, K., Hata, K., Li, E., and Jaenisch, R. (2003). Asynchronous replication timing of imprinted loci is independent of DNA methylation, but consistent with differential subnuclear localization. Genes Dev. *17*, 759–773.

Ho, T. H., Savkur, R. S., Poulos, M. G., Mancini, M. A., Swanson, M. S., and Cooper, T. A. (2005). Colocalization of muscleblind with RNA foci is separable from mis-regulation of alternative splicing in myotonic dystrophy. J. Cell Sci. *118*, 2923–2933.

Hu, J. F., Pham, J., Dey, I., Li, T., Vu, T. H., and Hoffman, A. R. (2000). Allele-specific histone acetylation accompanies genomic imprinting of the insulin-like growth factor II receptor gene. Endocrinology *141*, 4428–4435.

Huang, S., Deerinck, T. J., Ellisman, M. H., and Spector, D. L. (1994). In vivo analysis of the stability and transport of nuclear poly(A)+ RNA. J. Cell Biol. *126*, 877–899.

Jolly, C., Metz, A., Govin, J., Vigneron, M., Turner, B.M., Khochbin, S., and Vourc'h, C. (2004). Stress-induced transcription of satellite III repeats. J. Cell Biol. *164*, 25–33.

Katayama, S. *et al.* (2005). Antisense transcription in the mammalian transcriptome. Science *309*, 1564–1566.

Kedersha, N., and Anderson, P. (2002). Stress granules: sites of mRNA triage that regulate mRNA stability and translatability. Biochem. Soc. Trans. *30*, 963–969.

Kedersha, N., Stoecklin, G., Ayodele, M., Yacono, P., Lykke-Andersen, J., Fitzler, M. J., Scheuner, D., Kaufman, R. J., Golan, D. E., and Anderson, P. (2005). Stress granules and processing bodies are dynamically linked sites of mRNP remodeling. J. Cell Biol. *169*, 871–884.

Kiss, T. (2002). Small nucleolar RNAs: an abundant group of noncoding RNAs with diverse cellular functions. Cell *109*, 145–148.

Komine, Y., Tanaka, N. K., Yano, R., Takai, S., Yuasa, S., Shiroishi, T., Tsuchiya, K., and Yamamori, T. (1999). A novel type of non-coding RNA expressed in the rat brain. Brain Res. Mol. Brain Res. *66*, 1–13.

Lamond, A. I., and Spector, D. L. (2003). Nuclear speckles: a model for nuclear organelles. Nat. Rev. Mol. Cell Biol. *4*, 605–612.

Lawrence, J. B., Singer, R. H., and Marselle, L. M. (1989). Highly localized tracks of specific transcripts within interphase nuclei visualized by in situ hybridization. Cell *57*, 493–502.

Lin, S. P., Youngson, N., Takada, S., Seitz, H., Reik, W., Paulsen, M., Cavaille, J., and Ferguson-Smith, A. C. (2003). Asymmetric regulation of imprinting on the maternal and paternal chromosomes at the Dlk1-Gtl2 imprinted cluster on mouse chromosome 12. Nat. Genet. *35*, 97–102.

Mancini-Dinardo, D., Steele, S. J., Levorse, J. M., Ingram, R. S., and Tilghman, S. M. (2006). Elongation of the Kcnq1ot1 transcript is required for genomic imprinting of neighboring genes. Genes Dev. *20*, 1268–1282.

Mattick, J. S. (2004). RNA regulation: a new genetics? Nat. Rev. Genet. *5*, 316–323.

Melcak, I., Cermanova, S., Jirsova, K., Koberna, K., Malinsky, J., and Raska, I. (2000). Nuclear pre-mRNA compartmentalization: trafficking of released transcripts to splicing factor reservoirs. Mol. Biol. Cell 11, 497–510.

Miyoshi, N., Wagatsuma, H., Wakana, S., Shiroishi, T., Nomura, M., Aisaka, K., Kohda, T., Surani, M. A., Kaneko-Ishino, T., and Ishino, F. (2000). Identification of an imprinted gene, Meg3/Gtl2 and its human homologue MEG3, first mapped on mouse distal chromosome 12 and human chromosome 14q. Genes Cells 5, 211–220.

O'Neill, M. J. (2005). The influence of non-coding RNAs on allele-specific gene expression in mammals. Hum. Mol. Genet. 14(Spec No 1), R113–R120.

Perry, R. P., Kelley, D. E., and LaTorre, J. (1974). Synthesis and turnover of nuclear and cytoplasmic polyadenylic acid in mouse L cells. J. Mol. Biol. 82, 315–331.

Politz, J. C., and Pederson, T. (2000). Review: movement of mRNA from transcription site to nuclear pores. J. Struct. Biol. 129, 252–257.

Politz, J. C., Tuft, R. A., Pederson, T., and Singer, R. H. (1999). Movement of nuclear poly(A) RNA throughout the interchromatin space in living cells. Curr. Biol. 9, 285–291.

Pollard, K. S. et al. (2006). An RNA gene expressed during cortical development evolved rapidly in humans. Nature 443, 167–172.

Prasanth, K. V., Prasanth, S. G., Xuan, Z., Hearn, S., Freier, S. M., Bennett, C. F., Zhang, M. Q., and Spector, D. L. (2005). Regulating gene expression through RNA nuclear retention. Cell 123, 249–263.

Prasanth, K. V., Rajendra, T. K., Lal, A. K., and Lakhotia, S. C. (2000). Omega speckles—a novel class of nuclear speckles containing hnRNPs associated with noncoding hsr-omega RNA in Drosophila. J. Cell Sci. 113(Pt 19), 3485–3497.

Reik, W., and Walter, J. (2001). Genomic imprinting: parental influence on the genome. Nat. Rev. Genet. 2, 21–32.

Royo, H., Bortolin, M. L., Seitz, H., and Cavaille, J. (2006). Small non-coding RNAs and genomic imprinting. Cytogenet. Genome Res. 113, 99–108.

Schratt, G. M., Tuebing, F., Nigh, E. A., Kane, C. G., Sabatini, M. E., Kiebler, M., and Greenberg, M. E. (2006). A brain-specific microRNA regulates dendritic spine development. Nature 439, 283–289.

Schuster-Gossler, K., Bilinski, P., Sado, T., Ferguson-Smith, A., and Gossler, A. (1998). The mouse Gtl2 gene is differentially expressed during embryonic development, encodes multiple alternatively spliced transcripts, and may act as an RNA. Dev. Dyn. 212, 214–228.

Seidl, C. I., Stricker, S. H., and Barlow, D. P. (2006). The imprinted Air ncRNA is an atypical RNAPII transcript that evades splicing and escapes nuclear export. EMBO J. 25, 3565–3575.

Seitz, H., Royo, H., Bortolin, M. L., Lin, S. P., Ferguson-Smith, A. C., and Cavaille, J. (2004a). A large imprinted microRNA gene cluster at the mouse Dlk1-Gtl2 domain. Genome Res. 14, 1741–1748.

Seitz, H., Royo, H., Lin, S. P., Youngson, N., Ferguson-Smith, A. C., and Cavaille, J. (2004b). Imprinted small RNA genes. Biol. Chem. 385, 905–911.

Seitz, H., Youngson, N., Lin, S. P., Dalbert, S., Paulsen, M., Bachellerie, J. P., Ferguson-Smith, A. C., and Cavaille, J. (2003). Imprinted microRNA genes transcribed antisense to a reciprocally imprinted retrotransposon-like gene. Nat. Genet. 34, 261–262.

Shamovsky, I., Ivannikov, M., Kandel, E. S., Gershon, D., and Nudler, E. (2006). RNA-mediated response to heat shock in mammalian cells. Nature 440, 556–560.

Shen, R. Y., Altar, C. A., and Chiodo, L. A. (1994). Brain-derived neurotrophic factor increases the electrical activity of pars compacta dopamine neurons in vivo. Proc. Natl. Acad. Sci. USA 91, 8920–8924.

Sleutels, F., and Barlow, D. P. (2002). The origins of genomic imprinting in mammals. Adv. Genet. 46, 119–163.

Sleutels, F., Zwart, R., and Barlow, D. P. (2002). The non-coding Air RNA is required for silencing autosomal imprinted genes. Nature 415, 810–813.

Smith, C. M., and Steitz, J. A. (1998). Classification of gas5 as a multi-small-nucleolar-RNA (snoRNA) host gene and a member of the 5'-terminal oligopyrimidine gene family reveals common features of snoRNA host genes. Mol. Cell. Biol. 18, 6897–6909.

Thakur, N., Tiwari, V. K., Thomassin, H., Pandey, R. R., Kanduri, M., Gondor, A., Grange, T., Ohlsson, R., and Kanduri, C. (2004). An antisense RNA regulates the bidirectional silencing property of the Kcnq1 imprinting control region. Mol. Cell. Biol. 24, 7855–7862.

Tierling, S., Dalbert, S., Schoppenhorst, S., Tsai, C. E., Oliger, S., Ferguson-Smith, A. C., Paulsen, M., and Walter, J. (2006). High-resolution map and imprinting analysis of the Gtl2-Dnchc1 domain on mouse chromosome 12. Genomics 87, 225–235.

Tourriere, H., Chebli, K., Zekri, L., Courselaud, B., Blanchard, J. M., Bertrand, E., and Tazi, J. (2003). The RasGAP-associated endoribonuclease G3BP assembles stress granules. J. Cell Biol. 160, 823–831.

Tycowski, K. T., Shu, M. D., and Steitz, J. A. (1996). A mammalian gene with introns instead of exons generating stable RNA products. Nature 379, 464–466.

Verschure, P. J., van Der Kraan, I., Manders, E. M., and van Driel, R. (1999). Spatial relationship between transcription sites and chromosome territories. J. Cell Biol. 147, 13–24.

Visa, N., Puvion-Dutilleul, F., Harper, F., Bachellerie, J. P., and Puvion, E. (1993). Intranuclear distribution of poly(A) RNA determined by electron microscope in situ hybridization. Exp. Cell Res. 208, 19–34.

Wang, Y., Crawford, D. R., and Davies, K. J. (1996). adapt33, a novel oxidant-inducible RNA from hamster HA-1 cells. Arch. Biochem. Biophys. 332, 255–260.

Xing, Y., Johnson, C. V., Dobner, P. R., and Lawrence, J. B. (1993). Higher level organization of individual gene transcription and RNA splicing. Science 259, 1326–1330.

Yelin, R. et al. (2003). Widespread occurrence of antisense transcription in the human genome. Nat. Biotechnol. 21, 379–386.

Zamore, P. D., and Haley, B. (2005). Ribo-gnome: the big world of small RNAs. Science 309, 1519–1524.